2018

Impact of grassland conversion to forest on groundwater recharge in the Nebraska Sand Hills

Zablon A. Adane
University of Nebraska-Lincoln, ZABLON@HUSKERS.UNL.EDU

Paolo Nasta
University of Napoli Federico II, paolo.nasta@unina.it

Vitaly A. Zlotnik
University of Nebraska - Lincoln, vzlotnik1@unl.edu

David A. Wedin
University of Nebraska-Lincoln, dwedin1@unl.edu

Journal of Hydrology: Regional Studies 15 (2018) 171–183

Contents lists available at ScienceDirect

Journal of Hydrology: Regional Studies

journal homepage: www.elsevier.com/locate/ejrh

Impact of grassland conversion to forest on groundwater recharge in the Nebraska Sand Hills

Zablon A. Adane[a,d,*], Paolo Nasta[b], Vitaly Zlotnik[a], David Wedin[c]

[a] Department of Earth and Atmospheric Sciences, University of Nebraska-Lincoln, Lincoln, NE, USA
[b] Department of Agriculture, Division of Agricultural, Forest, and Biosystems Engineering, University of Napoli Federico II, Portici, Napoli, Italy
[c] School of Natural Resources, University of Nebraska-Lincoln, Lincoln, NE, USA
[d] World Resources Institute, Washington D.C., USA

ARTICLE INFO

Keywords:
Land-use change
Afforestation
High Plains Aquifer
Groundwater recharge
Numerical model

ABSTRACT

Study region: Nebraska National Forest in the High Plains Aquifer, Nebraska Sand Hills, U.S.A.
Study focus: This research aimed to investigate the effects of grassland conversions to forest on recharge rates in a century-old experimental forest. The DiffeRential Evolution Adaptive Metropolis ($DREAM_{ZS}$) global optimization algorithm was used to calibrate the effective soil hydraulic parameters from observed soil moisture contents for 220 cm deep uniform soil profiles. The historical recharge rates were then estimated by applying the numerical model HYDRUS 1-D for simulation of two plots representing grasslands and dense pine forest conditions.
New hydrological insights: The results indicate that conversion from grasslands to dense pine forests led to vegetation induced changes in soil hydraulic properties, increased rooting depth, and greater leaf area index, which together altered the water budget considerably. The impacts of land use change, expressed in percent of gross precipitation, include a 7% increase in interception associated with an increase in leaf area index, a nearly 10% increase in actual evapotranspiration, and an overall reduction of groundwater recharge by nearly 17%. Simulated average annual recharge rates decreased from 9.65 cm yr^{-1} in the grassland to 0.07 cm yr^{-1} in the pine plot. These outcomes highlight the significance of the grassland ecology for water resources, particularly groundwater recharge, in the Nebraska Sand Hills and the overall sustainability and vitality of the High Plains Aquifer.

1. Introduction

Over time, the ever-increasing alteration of landscapes and the exploitation of plants have provided various ecosystem services but also caused ill effects to the environment. For example, while the increase in agricultural lands and productivity in the last two centuries has increased the capacity to sustain unprecedented population growth, it has also caused extensive deforestation, soil erosion and degradation, desertification, loss of biodiversity, and depletion of groundwater resources.

Concerns over the magnitude of deforestation and its associated impact on global climate change has made it imperative to maintain current forest coverage and reduce net loss of forest area through reforestation and afforestation programs. Afforestation, reforestation, and natural forest expansion have reduced net loss of forest area from approximately 9 million hectares per year in the 1990s to 7.3 million hectares per year by 2005 (FAO, 2005a). Most afforestation programs, however, have not been undertaken through conversion of agricultural lands but at the expense of natural vegetation, particularly grasslands. In fact, vast areas of

* Corresponding author.
E-mail addresses: zablon@huskers.unl.edu (Z.A. Adane), paolo.nasta@unina.it (P. Nasta), vzlotnik@unl.edu (V. Zlotnik), dwedin1@unl.edu (D. Wedin).

https://doi.org/10.1016/j.ejrh.2018.01.001
Received 30 June 2017; Received in revised form 7 December 2017; Accepted 4 January 2018
Available online 05 February 2018

grasslands worldwide were found suitable for future forest restoration programs to offset anthropogenic CO_2 emissions (Bond, 2016).

In the last 100 years, natural regeneration and afforestation programs on various land uses have increased forest coverage (McCleery, 1992). Although forests provide several well documented ecosystem services (Nasi et al., 2002; Seppelt et al., 2011) a number of studies have also documented circumstances where conversions to forests have reduced streamflow (Brown et al., 2013), altered soil hydraulic properties (Kajiura et al., 2012), reduced soil moisture (James et al., 2003), and reduced recharge rates (Adane and Gates, 2015). The loss of soil moisture and groundwater recharge reductions have been attributed to the relatively higher evapotranspiration rates of the planted woody vegetation (Gates et al., 2011; Huang and Pang, 2011). Other studies have also partially associated these reductions in soil moisture and recharge rates to vegetation-induced soil water repellency (Adane et al., 2017) and greater rainfall interception of the introduced plantations (Allen and Chapman, 2001; Owens et al., 2006; Simic et al., 2014; Starks et al., 2014).

In the early-20th century, over 75% (215 million hectares) of the grassland coverage in the western United States was reported to be experiencing widespread degradation. In the Great Plains, most counties have lost at least part of their natural grassland vegetation (Klopatek et al., 1979). For instance, 85% to 95% of the native bluestem prairie vegetation in some areas had been converted to cropland (Sieg et al., 1999). The loss of grasslands has subsequently led to changes in the composition of vegetation, a loss of species diversity, and reductions in wildlife, such as the buffalo and prairie dogs in the Great Plains. While the Sand Hills grasslands are considered relatively intact at 85% of historical coverage, the region has experienced degradation related to conversion to cropland, habitat fragmentation, and overgrazing (FAO, 2005b). Changes in soils associated with grassland deterioration include a reduction in soil porosity, decrease in organic matter, and decrease in nutrient contents, as well as reductions in water-retention capacity (Burke et al., 1989). Such large-scale and rapid land use change has been known to cause significant changes to the environment including changes in hydrological regimes (Schilling et al., 2008; Spracklen and Garcia-Carreras, 2015), land degradation (Bruun et al., 2013; Ozalp et al., 2016), loss of habitat and wild life (Ochoa-Quintero et al., 2015), and contributing to climate change (Longobardi et al., 2016).

There is also a growing interest in the consequences of land use change on water resources at global, continental, and local scales (Elmhagen et al., 2015) with particular emphasis on groundwater recharge rates (recharge rates, for brevity) that feed shallow aquifers. Groundwater levels of many aquifers around the world have been decreasing over the last few decades due to excessive groundwater extraction for irrigation that surpasses groundwater recharge and replenishing rates (Scanlon et al., 2012; Terrell et al., 2002). The vulnerability of groundwater resources emphasizes the need to know reliable relationships between land use change and recharge rates, particularly in semi-arid regions where water scarcity is a critical concern. While the effect of natural vegetation conversion to agricultural land with respect to water resources has been well documented (Scanlon et al., 2007), studies on water resources impacts of other land use changes not associated with cropland are less common. In particular, the effect of grassland conversions to forests on water resources need further consideration due to the recent expansion of afforestation efforts and future forest restoration plans all over the world including in the United States (Adane and Gates, 2015; Eggemeyer et al., 2009; Huxman et al., 2005; Scanlon et al., 2009), China (Gates et al., 2011; Huang and Pang, 2011; Yang et al., 2012), and India (Calder et al., 1997).

This study evaluated the impact of land use change from grassland to forest on historical recharge rates in a century-old natural laboratory setting in the semi-arid Great Plains. HYDRUS 1-D was used to numerically simulate the plot-scale water balance at representative grassland and forest sites. The objectives of this study are: 1) to obtain effective soil hydraulic properties for the grass and dense pine profiles through inverse modeling using field observations, and 2) to evaluate the impact of grassland conversions to forests on recharge and the overall water budget.

2. Site description

The Nebraska National Forest (NNF) (Bessey Ranger District) is located in the south-central part of the Nebraska Sand Hills (NSH) and within the northern part of the High Plains Aquifer (Fig. 1; 41°51′45″N and 100°22′06″W; near Halsey, Nebraska, USA). The High Plains Aquifer covers an area of 450,000 km^2 and is ranked first in groundwater withdrawal for irrigation in the United States (Maupin and Barber, 2005; Scanlon et al., 2012). The NSH landscape is comprised mainly of eolian sand dunes that were deposited as recently as a few thousand years ago (Miao et al., 2007). The soil is approximately 92–97% sand (Wang et al., 2009) and that contributes to the greatest recharge rates in the High Plains Aquifer (Scanlon et al., 2012). The native vegetation of the NSH region consists of mixed-prairie grassland including little bluestem (*Schizachyrium scoparium*), switchgrass (*Panicum virgatum*), sand dropseed (*Sporobolus cryptandrus*), and Kentucky bluegrass (*Poa pratensis*) and is suitable to the historical land uses of ranching and cattle grazing (Eggemeyer et al., 2009). The climate is semi-arid continental with mean annual precipitation ranging between 40 and 70 cm yr^{-1} and potential evapotranspiration ranging between 30–136 cm yr^{-1} (Szilagyi et al., 2011).

The Nebraska National Forest is the largest man-made forest in the United States covering over 10,000 ha and it contains various coniferous tree species, which were planted as early as the 1930s (Hellerich, 2006). The forest is predominantly planted with ponderosa pine (*Pinus ponderosa*) and is surrounded by the native grassland ecosystem. The grass (G) plot with 10 m × 10 m dimensions is selected because the plot is the best approximation of the natural grassland conditions of the NSH within the forest (Fig. 1). The dense pine (DP) plot contains ponderosa pine trees at density rate of 700–1000 trees ha^{-1} and represents the dominant change in land use from the native grassland (Table 1). The selected dense pine plot contains the greatest pine tree plantation density of the entire forest. The forest also contains pine savannah and thinned pines plots with much less tree density that are thoroughly described in Adane and Gates (2015) and Adane et al. (2017).

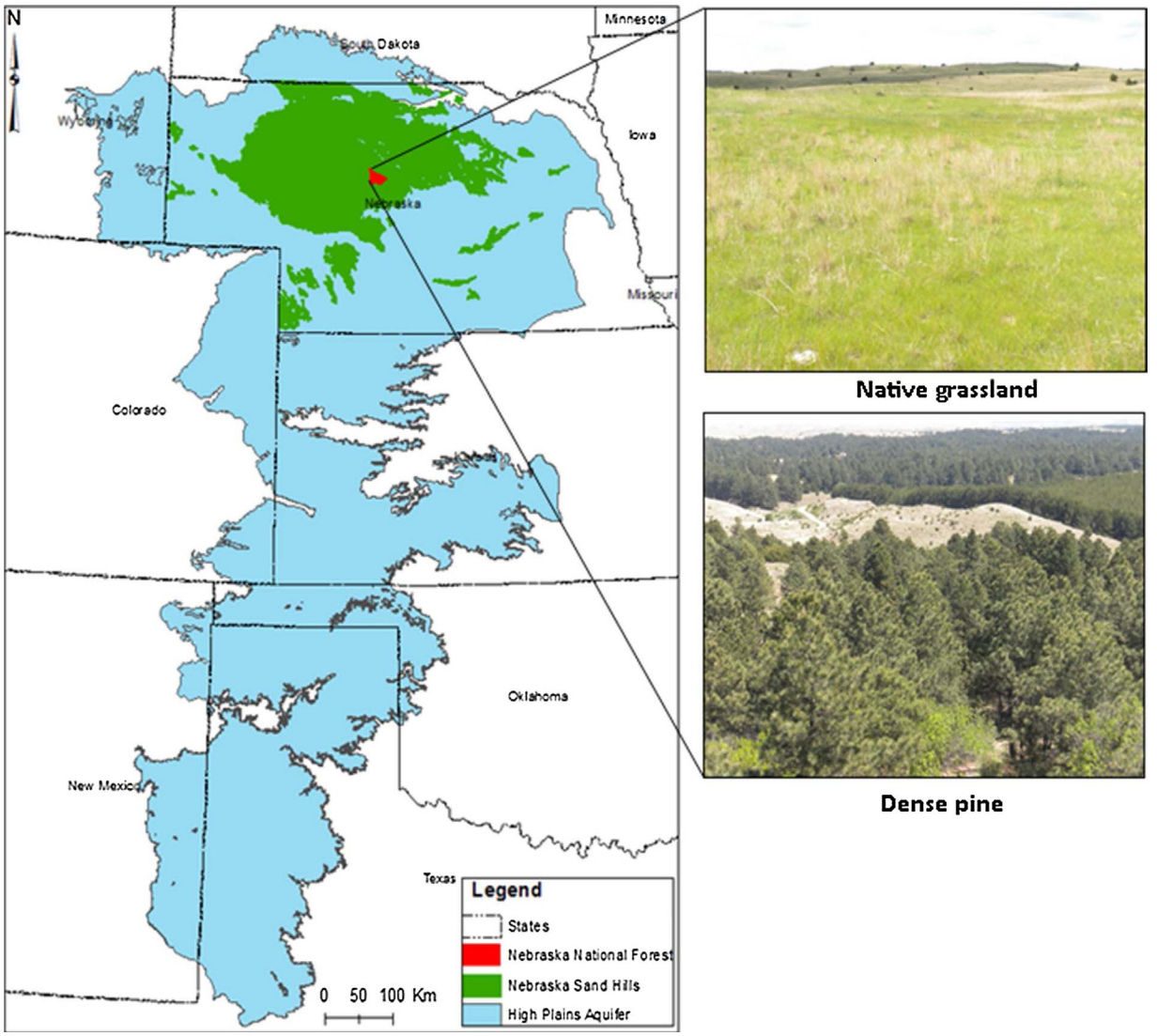

Fig. 1. Location map of the Nebraska National Forest, the Nebraska Sand Hills, and the High Plains Aquifer and images of the native grassland and dense pine forest land uses.

Table 1
Plot locations, vegetation type, elevations, and tree density.

Plot	Vegetation type	Longitude	Latitude	Elevation (m)	Tree density (trees ha^{-1})
G	Native grassland	100°21′16″	41°50′41″	860	–
DP	Dense pine	100°19′71″	41°51′69″	854	700–1000

3. Methods

3.1. Model conceptualization

HYDRUS 1-D (Šimůnek et al., 2008) was selected to simulate the water balance in the soil-plant-atmosphere system at the two plots (G and DP). HYDRUS 1-D numerically solves the one-dimensional water movement in the partially saturated soil domain. Fig. 2 illustrates the modeling approach and conceptualization. Climate forcing data inputs are historical precipitation (P) and reference potential evapotranspiration (ET_0). These atmospheric variables represent the climate inputs that are the same for all land use types. The impact of specific vegetation cover on P and ET_0 depends on crop coefficient (K_c) and leaf area index (LAI). While K_c converts ET_0 into specific crop potential evapotranspiration (ET_p), LAI determines rainfall interception (I) and the partitioning of ET_p into potential

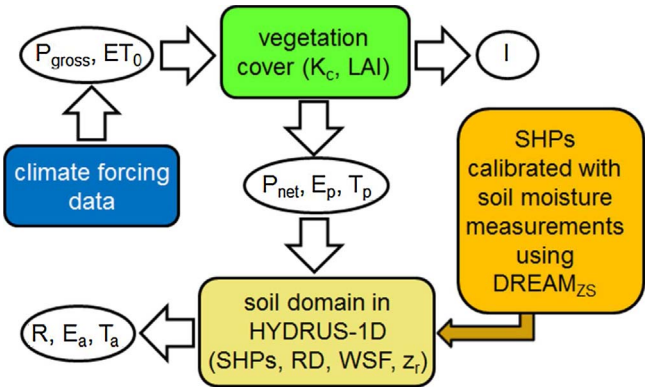

Fig. 2. Schematic overview of the modeling approach adopted in this study.

evaporation (E_p) and potential transpiration (T_p). Given the effect of foliage interception, gross (P_{gross}) and net (P_{net}) precipitation are differentiated in the remainder of this paper. Prior to running model simulations, it is necessary to set up the soil hydraulic properties (SHPs), root distribution (RD), water stress function (WSF) parameters and maximum root depth (z_r) for each specific vegetation type. In this study, the HYDRUS database default RD was applied where maximum root distribution is at the soil surface and minimum is at the bottom of soil profile. Maximum root depth was assumed to be 50 cm for grass and 200 cm for the pine tree, respectively. The SHPs were calibrated through inverse modeling by using sporadic daily measurements of soil moisture contents. Calibration was performed by using a global-optimization tool, namely $DREAM_{ZS}$ (Vrugt, 2016), by minimizing the discrepancy between observed and simulated daily values of soil moisture. The output fluxes are given by actual evaporation (E_a), actual transpiration (T_a) and water drainage at the bottom of the soil profile, assumed as groundwater recharge (R).

3.2. Field measurement methods and available data basis

3.2.1. Historic climate records

Climate data output from the ensemble CMIP5 ESM was obtained from the CMIP5 Modeling Groups for the historical period 1950–2000. The dataset included daily precipitation and minimum and maximum daily temperatures at 1/8th degree downscaled resolution (12 km × 12 km area) for the (41°45′0″N, 41°52′30″N) latitude and (100°30′0″W, 100°22′30″W) longitude bounds encompassing the NNF. The reference potential evapotranspiration (ET_0) was calculated using the Hargreaves equation (Hargreaves and Allen, 2003) whilst precipitation is defined as gross precipitation (P_{gross}).

3.2.2. Leaf area index

The Leaf Area Index (LAI) was measured for both the grassland and the dense pine plots. The LAI for the evergreen dense pine plot was determined to be 1.9 using hemispheric camera 360° images with Ellipsoid-Campbell calculation method (Hellerich, 2006; Robbins, 2005). This value was assumed as time-invariant throughout the year. The forest was planted in areas where the dense pine forests exist in non-contiguous patches in a grassland setting. The forest also contains parts that are pine savannah, thinned pine, and mixed vegetation patches with sparse pine trees with much lower average LAI values ranging from 0.6 to 1.9 (Adane et al., 2017). LAI values of the grasslands were obtained approximately once every month through a destructive method where grass leaves removed from representative 0.25 m × 0.25 m quadrant sub-plots were scanned using LI-3100 leaf area meter (LI-COR, Lincoln, NE, U.S.A) in the laboratory. The scanned cumulative grass leaf area divided by the area of each sub-plot represents the plot level LAI values (He et al., 2007; Bréda, 2003). The dataset included 66 data points spanning over 11 years of collection (2005–2015). Interpolations of the grassland daily LAI values were given by a second-order polynomial function (day of year, DOY) during the growing season (Nasta and Gates, 2013):

$$LAI = \begin{cases} 0 & 0 < DOY < 101 \\ -8.88 \times 10^{-5} DOY^2 + 0.0368 DOY - 2.77 & 100 < DOY < 319 \\ 0 & 318 < DOY < 366 \end{cases} \quad (1)$$

The observed and interpolated (Eq. (1)) daily LAI values for the Sand Hills grasses are depicted in Fig. 3. Measured LAI is approximately 0 in the cold winter and early spring (~0 to 100 and 319–365 days), increases in the spring until it peaks at about 1.3 in the summer and early fall months of June to September (~150 to 270 days) and subsequently declines to 0 in late October.

3.2.3. Soil moisture data

The Time Domain Reflectometry (TDR) soil moisture daily measurements were collected once a month in both the grassland and dense pine plots using IMKO T3 probe (IMKO Micromodultechnik GmbH, Ettlingen, Germany). The TDR instrument was calibrated to the local sandy soil properties. The plot profiles extended to 220 cm depth at approximately 20–30 cm intervals and data collected from March 2005 to January 2012 were used in this study. The historic record contained some missing data due to sensor malfunction

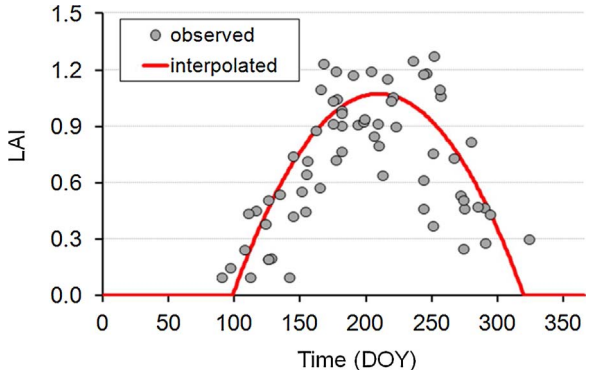

Fig. 3. Observed and interpolated LAI values as a function of time (DOY) for the Sand Hills grasses.

and maintenance. This resulted in a total of 66 readings over the span of 7 years that was used in model calibration and validation.

3.3. Hydrological model

3.3.1. Model set up

The water fluxes in the soil-plant-atmosphere system are simulated using the HYDRUS 1-D software package (Šimůnek et al., 2008), which numerically solves the one-dimensional Richards equation for variably-saturated soil moisture flow:

$$\frac{\partial \theta}{\partial t} = \frac{\partial}{\partial z}\left\{K\left[\left[\frac{\partial h}{\partial z}+1\right]\right]\right\} - \zeta \tag{2}$$

where t [T] is time, z [L] is the vertical coordinate, h [L] is the water pressure head, θ [$L^3\,L^{-3}$] is the soil volumetric water content, K [$L\,T^{-1}$] is the hydraulic conductivity and ζ [$L^3\,L^{-3}\,T^{-1}$] is the sink term function that describes volumetric macroscopic root water uptake. The units adopted in this paper are day (d) and centimeter (cm) for the dimensions of time (T) and length (L), respectively. The soil water retention function $\theta(h)$ is described by van Genuchten's equation (van Genuchten, 1980):

$$h = \theta_r + \frac{\theta_s - \theta_r}{[1 + (\alpha h)^n]^m} \tag{3}$$

with Mualem's condition (Mualem, 1976):

$$m = 1 - \frac{1}{n} \tag{4}$$

where α (cm^{-1}), m (−) and n (−) are shape parameters, θ_r ($cm^3\,cm^{-3}$) and θ_s ($cm^3\,cm^{-3}$) are residual and saturated water contents, respectively. Using degree of soil saturation, S_e, which varies from 0 at ($\theta = \theta_r$) to 1 at ($\theta = \theta_s$), an expression for the unsaturated hydraulic conductivity function $K(S_e)$ is given by:

$$K(S_e) = K_s S_e^{\tau}[1 - \{1 - S_e^{1/m}\}^m]^2 \;;\; S_e = (\theta - \theta_r)/(\theta_s - \theta_r) \tag{5}$$

where K_s ($cm\,d^{-1}$) is saturated hydraulic conductivity, τ (−) is the tortuosity parameter, assumed to be $\tau = 0.5$ (Mualem, 1976). The potential evapotranspiration ET_p referred to the specific vegetation type is calculated by multiplying ET_0 by the specific crop coefficient, K_c. Subsequently ET_p is partitioned into potential evaporation, E_p ($cm\,d^{-1}$) and potential transpiration, T_p ($cm\,d^{-1}$) according to the following empirical equation:

$$E_p = ET_p \cdot e^{-k \cdot LAI} \tag{6}$$

where κ (−) is the dimensionless extinction coefficient for global solar radiation inside the canopy and is assumed to be equal to 0.463 (Ritchie, 1972), whereas LAI is the leaf area index assumed to be steady (LAI = 1.9) for the pine and time-variant for the grass (Eq. (1)). The rainfall interception I ($cm\,d^{-1}$) is calculated according to Braden (1985) and Schwärzel et al. (2006):

$$I = a \cdot LAI\left(1 - \frac{1}{1 + b \cdot P/a \cdot LAI}\right) \tag{7}$$

where a ($cm\,d^{-1}$) is an empirical coefficient, assumed to be 0.025 $cm\,d^{-1}$ and b (−) denotes the soil cover fraction given by:

$$b = 1 - e^{-k \cdot LAI} \tag{8}$$

Interception is subtracted from the gross precipitation (P_{gross}) in order to obtain the net precipitation (P_{net}) that falls to the soil surface. The soil profile which extends to 220 cm depth (maximum depth of direct measurements of soil moisture), is considered homogeneous over a single uniform layer with a set of "effective" soil hydraulic properties (e.g., Nasta and Romano, 2016). Net precipitation and potential evaporation represent the system-dependent atmospheric upper boundary conditions, whereas free

drainage is assumed at the lower boundary of the soil profile and is considered potential groundwater recharge (R) in this study. Direct measurements of soil moisture values along the vertical dimension at initial time step of model simulation represent the initial condition. The term T_p determines the potential root water uptake, $\zeta(h)$, which is reduced through the Feddes condition (Feddes et al., 2001). Two simulations are set up in HYDRUS 1-D: a) grass with K_c = 0.95 and 50 cm root depth; and b) pine with K_c = 1.0 and 200 cm root depth. The Feddes parameters were retrieved from the database available within in HYDRUS 1-D.

3.3.2. Model calibration and validation

For each of the two simulations, the effective soil hydraulic parameters featuring in van Genuchten's relations (Eqs. (3)–(5)) are unknown and need to be estimated by inverse modeling. The robustness of any optimization algorithm used for inverse modeling often determines its suitability for specific parameter estimation. The first optimization routines were the local-search algorithms, such as the least-square estimators like the one embedded in HYDRUS 1-D. The results in these algorithms strongly depend on the initial guesses of each parameter value, thus facing a high risk of early termination and failure in multiple-local minima (Vrugt et al., 2003).

In order to eliminate the dependence on the parameter initial guesses, there have been a series of robust global search algorithms to optimize soil hydraulic parameters. One of the most popular techniques proposed in the scientific literature, the DiffeRential Evolution Adaptive Metropolis algorithm (DREAM_{ZS}) coupled to the efficient Markov-chain Monte-Carlo sampling scheme (Laloy and Vrugt, 2012; Vrugt, 2016; Vrugt et al., 2008) is adopted in this study because a Bayesian interpretation is more appropriate in order to infer "the most probable" set of parameters and their corresponding uncertainties (Moradkhani et al., 2005). The Bayesian statistical inference combines the data likelihood with a priori distribution to derive the posterior probability density functions of the model parameters. The objective function $\Phi(\boldsymbol{P})$ to be minimized in the optimization routine is defined as the root mean squared deviation (RMSD), which quantifies the discrepancy between observed and simulated soil moisture values:

$$\min_P \Phi(\boldsymbol{P}, z) = \sqrt{\frac{\sum_{t=1}^{t_{TOT}} \sum_{z=1}^{z_{TOT}} [\theta_{TDR}(z, t) - \theta_{SIM}(z, t, \boldsymbol{P})]^2}{t_{TOT} + z_{TOT} - 1}} \tag{9}$$

where the vector $\boldsymbol{P} = (\theta_r, \theta_s, \alpha, n,$ and $K_s)$ contains the optimization parameters, and the subscripts *TDR* and *SIM* denote the observed and simulated soil water content values corresponding to soil depth z at observation time t for 66 days between 2005 up to 2012 at approximately one daily record per month. Maintenance months, where data were not collected and data points that are unrealistically high, were not considered.

HYDRUS 1-D model was implemented in DREAM_{ZS} using the MATLAB environment. The minimum and maximum bounds for the grass profile soil hydraulic parameters were selected based on field data for Valentine sand (unpublished), pedotransfer function (Kettler et al., 2001) and global sand textures reported by Carsel and Parish (1988). The soil hydraulic property bounds for the pine profile were further broadened in order to account for the impact of soil hydrophobicity (Adane et al., 2017). Ranges are shown in Table 2. The main MATLAB text file (SELECTOR.IN) is automatically updated within the program with a new set of the five hydraulic parameters ($\theta_r, \theta_s, \alpha, n,$ and K_s) that have to be optimized, whereas the simulated water content values for each observation z-depth and each time step t are retrieved from the text file (Obs_Node.Out).

The number of observed water contents were 660 in total and were recorded at 10 different depths and in 66 days (distributed over 7 years). A vector of 370 observed water content values (10 depths in 37 days collected over 4 years) were used for calibration (2005–2008) and the remaining 290 (10 depths in 29 days collected over 3 years) were used for model validation (2009–2011). The performance diagnostic is quantified through the root mean squared deviation (RMSD) according to Eq. (9).

4. Results

4.1. Soil moisture

The soil moisture content was generally greater in the grassland plot soil profile than in the dense pine plot. The total average moisture content for the grassland plot profile was approximately 13% ranging from 11.3% to 17.2%. The DP plot soil profile was drier compared with the G plot with the soil moisture content averaging approximately 9% and the average for each depth interval ranging from 8.3% to 12.7% over the 7-year dataset. The G plot profile had greater overall average soil moisture content for each

Table 2
Minimum and maximum bounds used for soil hydraulic property optimization.

Parameter	Units	Grass		Pine	
		Min	Max	Min	Max
θ_r	$cm^3\,cm^{-3}$	0.03	0.045	0.02	0.045
θ_s	$cm^3\,cm^{-3}$	0.35	0.43	0.30	0.43
α	cm^{-1}	0.03	0.145	0.01	0.145
n	[–]	1.65	3.0	1.0	3.0
K_s	$cm\,d^{-1}$	200	750	100	750

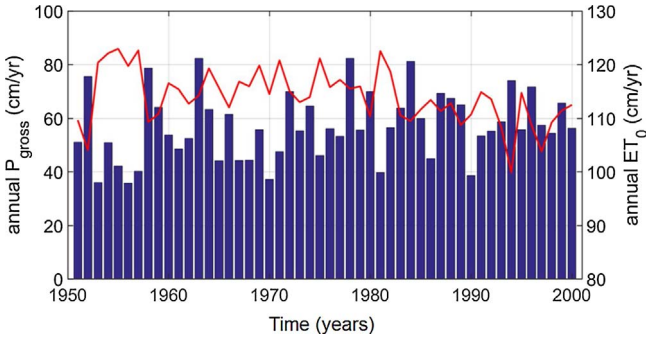

Fig. 4. Historical trends in annual averages of gross precipitation (P_{gross}) and reference potential evapotranspiration (ET_0).

depth interval by approximately 48% to 84%. Gravimetric measurements taken from soil profile cores in 2012 suggest that the average soil moisture contents were 8.4% for the grass and 4.5% for the dense pine profiles (Adane and Gates, 2015), however, the low moisture values may also be partially attributed to the fact that 2012 was one of the driest years on record.

4.2. Historical climate trend

The average annual precipitation for the 1950–2000 time period was approximately 57.0 cm yr^{-1}, with the minimum of 35.8 cm yr^{-1} and the maximum of 82.3 cm yr^{-1} occurring in 1955 and 1977, respectively. The annual historical precipitation data also deviated from the mean by approximately 12.5 cm yr^{-1}. The decadal averages of the historical precipitation data suggest an increase in precipitation from approximately 53 cm yr^{-1} in the 1950s to 60 cm yr^{-1} in the 1990s. The reference potential evapotranspiration rate estimates were substantially greater than the annual precipitation with an average of 114.0 cm yr^{-1} and standard deviation of about 5.0 cm yr^{-1}. Fig. 4 illustrates the historical trends in annual averages of gross precipitation and reference evapotranspiration between 1950 and 2000.

4.3. Model calibration and validation results

The calibration results comparing the observed and simulated soil moisture data subjected to observed net precipitation (P_{net}) and potential evapotranspiration (ET_p) daily values are depicted in Fig. 5. Ten observed (black stars) θ-values corresponding to each soil depth are reported at each time step while the gray bands signify the modeled θ-values of the uniform soil profile corresponding to posterior probability density functions of the effective soil hydraulic parameters.

The most probable values of the three estimated effective soil hydraulic parameters correspond to the median-values of their posterior frequency distributions and are reported in Table 3. The θ_r and θ_s parameter estimates for the grass and dense pine profiles

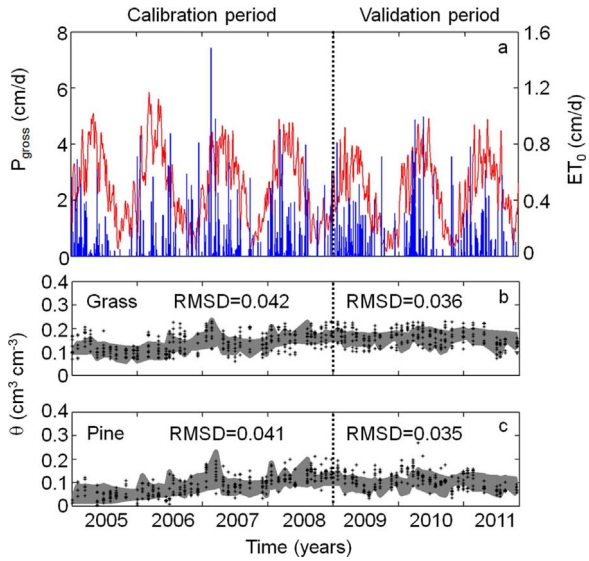

Fig. 5. Calibration (2005–2008) and validation (2009–2011) results comparing the observed and simulated soil moisture data: (a) precipitation (blue) and potential evapotranspiration (red) in cm·d-1 for 2005–2011; (b) observed (black stars) and simulated (gray uncertainty bands) soil moisture content for the grass plot, and (c) observed (black stars) and simulated (gray uncertainty bands) soil moisture content for the dense pine plot.

Table 3
The most probable values of the three optimized parameters.[a]

Parameter	Units	Grass	Pine
θ_r	$cm^3\,cm^{-3}$	0.041 (6.7%)	0.021 (42.8%)
θ_s	$cm^3\,cm^{-3}$	0.43 (1.9%)	0.32 (6.9%)
α	cm^{-1}	0.077 (36.1%)	0.011 (14.2%)
n	[–]	1.65 (1.3%)	1.36 (3.4%)
K_s	$cm\,d^{-1}$	214.1 (31.9%)	186.7 (28.9%)

[a] Associated coefficients of variation, CV are reported in parentheses.

were 0.041 and 0.021 and 0.43 and 0.32, respectively. The α parameter results were 0.077 cm^{-1} and 0.011 cm^{-1}, while the n parameter results were 1.65 and 1.36 for the grassland and dense pine plot soil profiles, respectively. One of the most uncertain parameters in this optimization for both grassland and dense pine soil profiles was K_s with values of 218 $cm\,d^{-1}$ and 185 $cm\,d^{-1}$ respectively. Since the study site generally consists of homogenous Valentine sands, the optimized K_s values are reasonable and are consistent with unpublished field data (K_s = 240 $cm\,d^{-1}$), despite being much lower than the K_s = 713 $cm\,d^{-1}$ reported for a global sand texture in Carsel and Parish (1988). While the coefficients of variation (CV) indicate greater confidence in the θ_r, θ_s, and n parameter (6.7%, 1.9%, and 1.3%) estimates, uncertainties were greater for α (CV = 36.1%) and K_s (31.9%) parameters (Table 3). The coefficients of variation were also notably greater for the pine profile and suggest that while the overall calibration is robust, it could be improved by refining individual parameter estimates. It is important to note that approximations applied in the model, such as uniform soil profile, estimated root depth and root distribution coupled with a coarse (sporadic and at times non-contiguous) temporal resolution of daily observed soil moisture content data can generate "epistemic" errors and uncertainties (Nasta and Romano, 2016). The model simulations were essentially able to reproduce the hydrological dynamics and trends of the observed soil moisture contents in both vegetation plots reasonably well. The RMSD values were relatively low (4.2% and 3.6% in the calibration and validation periods, respectively) for the grassland plot (Fig. 5b). Similarly, the dense pine plot soil moisture content calibration and validation processes resulted in low RMSD of 4.1% and 3.5%, respectively (Fig. 5c). Considering the calibrations were done based on a set of limited data, the optimization was reasonably robust, even though previous investigations have reported more robust performances (Wöhling and Vrugt, 2011).

4.4. Simulated historical recharge rate and water budget results

Fig. 6 shows the average annual balance in terms of P_{gross} percentages whereas Tables 4 and 5 report the summary statistics of annual average water balance components for grass and pine, respectively. The average annual gross precipitation for the 1950–2000 time period was 57.0 $cm\,yr^{-1}$ for the area. The estimated vegetation canopy interception of gross precipitation was approximately 1.3 $cm\,yr^{-1}$ in the grassland and 5.6 $cm\,yr^{-1}$ in the dense pine plots and accounted for approximately 2.2% and 9.9% of gross precipitation, respectively.

The grass potential evapotranspiration (ET_p) is lower than the pine because of the marginal effect of K_c (K_c = 0.95 for the grass and K_c = 1 for the pine) and the considerable impact of LAI on T_p, which is null for the grass plot during the dormant season.

The average annual actual evapotranspiration estimates were 45.9 $cm\,yr^{-1}$ in the grass to 51.4 $cm\,yr^{-1}$ for the dense pine plots. The averages of total actual evapotranspiration rates represented 81% and 90% of the gross precipitation in the grass and dense pine profiles, respectively. These estimates are consistent with the results of Szilagyi et al. (2011) that reported the ponderosa pine plantations in the NNF evaporated 5% to 10% more than the average annual precipitation. The average recharge rate estimates were 9.7 $cm\,yr^{-1}$ for the grass and 0.07 $cm\,yr^{-1}$ for the dense pine plots, which represent 17% and 0.13% of gross precipitation, respectively.

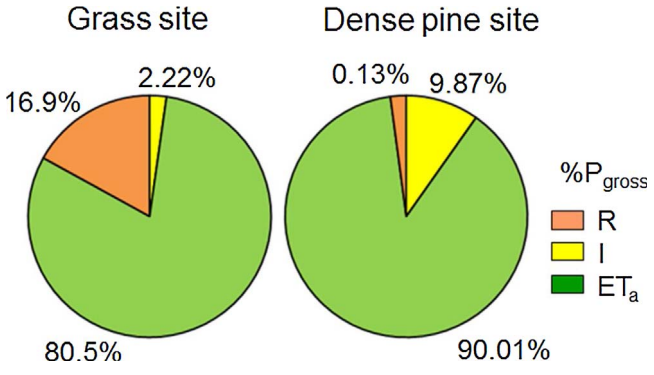

Fig. 6. Pie charts of water balance output components (I, R and ET_a) in terms of P_{gross} percentages for the grass (pie chart on the left) and pine (pie chart on the left) sites.

Table 4
Summary statistics (mean, standard deviation, coefficient of variation, minimum and maximum are denoted by μ, σ, CV, Min and Max, respectively) of historical average of climate and simulated water balance data at the grass plot.

	I cm yr^{-1}	P_{net} cm yr^{-1}	ET_p cm yr^{-1}	ET_a cm yr^{-1}	R cm yr^{-1}
μ	1.27	55.77	78.74	45.94	9.65
σ	0.21	12.35	3.75	6.60	6.52
CV	16.56	22.14	4.76	14.36	67.54
Min	1.82	80.86	86.09	59.20	33.25
Max	0.85	34.89	69.77	31.20	1.38

Table 5
Summary statistics (mean, standard deviation, coefficient of variation, minimum and maximum are denoted by μ, σ, CV, Min and Max, respectively) of historical average of climate and simulated water balance data at the pine plot.

Pine plot	I cm yr^{-1}	P_{net} cm yr^{-1}	ET_p cm yr^{-1}	ET_a cm yr^{-1}	R cm yr^{-1}
μ	5.63	51.51	113.99	51.38	0.07
σ	0.60	12.07	5.04	10.98	0.25
CV	10.71	23.43	4.42	21.37	335.89
Min	4.26	31.02	99.81	30.80	0.02
Max	7.17	76.64	122.95	75.94	1.77

5. Discussion

5.1. Comparison with recharge studies in the Sand Hills

The historical recharge rate estimates were generally consistent with other field and modeled studies in the Nebraska Sand Hills. The average historical recharge rate estimated for the grasslands in this study was approximately 9.65 cm yr^{-1} and 17% of precipitation and is close to the results of Crosbie et al. (2013), which estimated 10–15 cm yr^{-1} and 20–30% of annual precipitation. The recharge estimates for the grasslands were also consistent with Scanlon et al. (2012) that reported a range of 2.5 cm yr^{-1} to 21.0 cm yr^{-1} for an average of 9.2 cm yr^{-1} for the Sand Hills in the Northern High Plains. While Szilagyi et al. (2011) estimated recharge rates to range between 3.7 and 4.9 cm yr^{-1}, an improved model in Szilagyi et al. (2011) estimated an average rate of 7.3 cm yr^{-1}. Billesbach and Arkebauer (2012) also reported 11.5 ± 2.0 cm yr^{-1} for a grazed grassland site with no plantations, located approximately 110 km from the present study site. A chloride mass balance study used to corroborate the remote sensing results estimated 10.3 cm yr^{-1} for a sampling location closest to this study area near Halsey, NE (Szilagyi et al., 2011). A study using soil moisture network data inverse modeling at Halsey estimated an annual recharge rate of 5.0 cm yr^{-1} and 7.1% of precipitation (Wang et al., 2016). A chloride mass balance and sulfate mass balance recharge study for the same plot used in this study also estimated 3.7 cm yr^{-1} and 10.0 cm yr^{-1}, respectively for the grasslands (Adane and Gates, 2015). However, the study conducted in the middle of a severe drought in 2012 contained considerably lower soil moisture contents compared to the long term soil moisture data obtained from TDR measurements and can potentially affect the final estimates of recharge. A study that used chemical tracers, (McMahon et al., 2006) estimated that recharge rates for the Sand Hills grassland can exhibit a broad range between 0.02 cm yr^{-1} to 7.0 cm yr^{-1}. While there have been a number of recharge studies in the Sand Hills, the range of estimates can still vary drastically because of spatial differences in precipitation and temperature gradient. As such, careful considerations of averaged values and thoughtful geographical partitioning of the NSH will provide more valuable information on recharge rates and the water balance.

Whereas few recharge estimates were available for the grasslands, estimates for the dense pine plantations have been even rarer. This study estimated almost negligible (0.07 cm yr^{-1}) average historical recharge rates for the dense pine plot. This result is consistent with the chloride mass balance method where Adane and Gates (2015) estimated the average recharge rate beneath the dense pine plot at approximately 0.7–1.0 cm yr^{-1}. In reference to the dense ponderosa pine plantation in the NNF, Szilagyi et al. (2011) reported that the plantations may evaporate more than annual precipitation suggesting that the recharge rate beneath the dense pine plantations may likely be negligible. In a temperate climate in south Western Australia, Farrington and Bartle (1991) estimated recharge beneath pines (*Pinus pinaster*) was 11.4 cm (15% of precipitation) but still 35% less than the adjacent woodlands. In the semi-arid Mediterranean climate in Spain, Bellot et al. (1999) also estimated recharge beneath pine trees to be negligible. Sharma et al. (1983) in Australia reported that conversion from grassland to pines (*Pinus radiata*) resulted in negligible recharge rates. Similarly, Holmes and Colville (1970a, b) documented that conversion recharge rates beneath grasslands (6.3 cm yr^{-1}) were reduced to 0 cm yr^{-1} beneath 24-year-old pines.

The severity of reduction in recharge is influenced by the plantation density of the pine trees. Adane and Gates (2015) reported that, compared to the native grassland, recharge beneath the sparse pine trees (LAI = 0.3) was only reduced by 14%. In the meantime, recharge beneath the pine savannah (LAI = 1.7) and dense pine trees (LAI = 2.2) were reduced by 51% and 73%, respectively. Comparing thinned and unthinned loblolly pine stands, Stogsdili et al. (1992) found that increased moisture in the soil

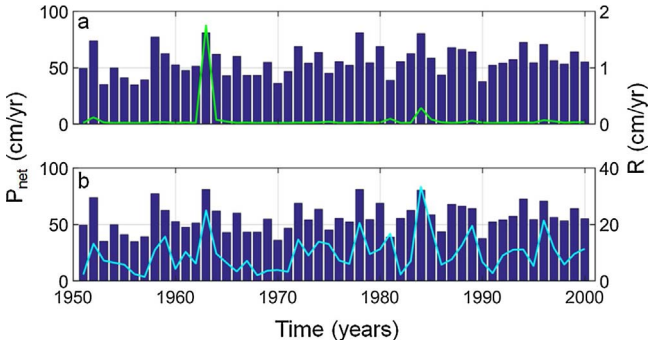

Fig. 7. Annual recharge rates (lines) compared to annual net precipitation rates (blue bars) for a) grass (green line) and b) dense pine (cyan line) plots.

profile is more a function of reduced leaf interception loss and increased throughfall rather than reduced water use from the tree stands. In addition to tree water use, understory vegetation, climate, and soil type play important roles on the severity of recharge reduction.

5.2. The impact of land use change on recharge and the soil water balance

The annual recharge rates for the grassland and dense pine profiles from 1950 to 2000 are shown in Fig. 7. The impact of land use change on recharge rates and water balance was assessed through the difference between the native grassland and the dense pine plots, indicating the change in the historical land use. This change included an increased root depth from 50 cm in the grassland to 200 cm in the pine vegetation, as well as increased canopy cover where the LAI ranged from 0 to 1.2 in the grasses and 1.87 for the evergreen dense ponderosa pines.

These changes to the land use have increased average interception more than fourfold from 1.3 cm yr^{-1} to 5.4 cm yr^{-1}, which are equivalent to 2.3% and 9.0% of gross precipitation. Such increase in canopy interception in trees is consistent with what has been reported by (Bosch and Hewlett, 1982), who found that canopy interception of 10% to 40%, which was considerably less than the 25–40% reported for coniferous trees in the UK (Calder, 2003), 19.4% for pines in Nepal (Ghimire et al., 2012), and 17% in semi-arid pine forest in Portugal (Valante et al., 1997). The conversion from grassland to dense pine vegetation also increased actual evapotranspiration from 45.9 cm yr^{-1} to 51.4 cm yr^{-1}, which agrees with the conclusions of Zhang et al. (2001), who reported that greater evapotranspiration in forests than pasture for semi-arid regions with less than 60.0 cm yr^{-1} precipitation. The average annual actual evapotranspiration including interception losses accounted for approximately 83% of the average gross precipitation in the grass plot and approximately 100% in the dense pines profiles, which are consistent with studies that estimated 90% in semi-arid climates (Huxman et al., 2005). Szilagyi et al. (2011) also estimated that evapotranspiration rates may exceed annual precipitation by up to 10% in the dense ponderosa pine of the NNF. The average transpiration rates were 16.1% greater in the dense pine plot (21.8 cm yr^{-1}) than in the grasses (18.3 cm yr^{-1}), which is a conclusion consistent with other studies (Zhang et al., 2001; Bosch and Hewitt, 1982). The actual evaporation estimate was also 13.4% greater in the dense pine (29.4 cm yr^{-1}) than in the grassland (25.3 cm yr^{-1}) profile, possibly in response to a 15% reduction experienced in soil hydraulic conductivity of the dense pine plot. The results are consistent with Allen and Chapman (2001) and Calder and Newson (1980) who reported the rate of extra water loss by evaporation in forests is much more efficient than grasslands due to turbulent winds generated by trees. Greater evaporation losses in the dense pine plot may also likely be due to longer exposure to radiation and the atmosphere compared to the grassland. Conversely, greater evaporation rates in grasses than trees have also been reported in Kelliher et al. (1993), where annual average evaporation rates were 0.46 cm day^{-1} compared to 0.40 cm day^{-1} in the coniferous trees likely due to the greater canopy cover of forests. Subsequently, land use change through grassland afforestation has reduced the average historical recharge rate by approximately 100% from 19.65 cm yr^{-1} to 0.07 cm yr^{-1} and was in agreement with the results of Adane and Gates (2015), who reported reductions up to 90% for the same study site. The recharge rate has also been reduced from 16.9% of precipitation in grasslands to 0.13% in the dense pine.

5.3. Sensitivity of groundwater recharge to maximum rooting depth

Root depth (z_r) determines how deep plants can access moisture in the soil profile. Thus, root depth has substantial influence on groundwater recharge and actual transpiration. A sensitivity analysis was performed to evaluate the impact of changing z_r on recharge. The results indicate that groundwater recharge rate sensitivity to root depth was greater in the grassland plot than the dense pine (as can be seen in Fig. 8).

While both plots are sensitive to rooting depth, it is important to note that recharge rates beneath the dense pine plot were considerably lower in general and practically negligible when maximum rooting depth exceeds 150 cm. Meanwhile, increasing rooting depth to 220 cm reduced groundwater recharge by 14 cm in the grass plot. If the grassland z_r is altered from the original value (50 cm) to either 100 cm or 10 cm, R decreases by 39% and increases by 58%, respectively. It is also noteworthy that the grass plot with rooting depth at 220 cm produced more simulated groundwater recharge than the dense pines with extremely shallow (10 cm)

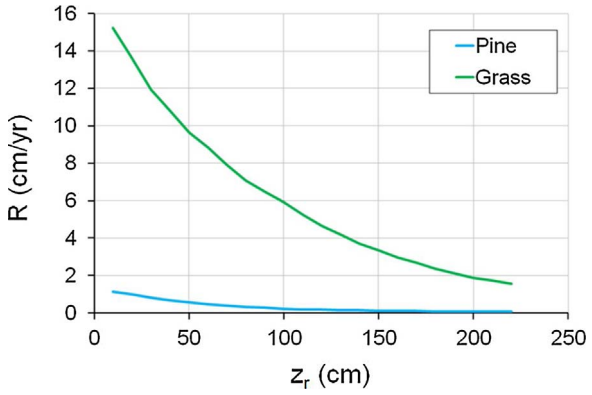

Fig. 8. Sensitivity of annual recharge rates to maximum root depth (z_r) for grass (green line) and pine (cyan line).

maximum rooting depth, which further highlights the significance of the grassland ecology in the Nebraska Sand Hills.

6. Conclusion

This study was among a very few site-specific investigations that evaluated the impact of land use change on recharge rates in the Nebraska Sand Hills. This study quantified the considerable impact that land use change has on recharge rates and overall water balance. The conversion from the historical native grassland to forested land reduced recharge rate by approximately 17% relative to gross precipitation. The actual evapotranspiration rates of the dense forest profile were also substantially greater than the grassland in response to increased canopy cover and greater root extinction depth. The results of a sensitivity analysis indicate that groundwater recharge rate sensitivity to root depth was greater in the grassland plot than the dense pine. Evaporation rate was also greater under the dense pine profile, partly due to lower saturated hydraulic conductivity value and longer exposure to ambient temperature and atmospheric demand.

Proper consideration needs to be given to the intrinsic uncertainties in the data, the simulations, and the parameter assumptions. The numerical model simulations did not consider the impact of preferential flow, discretized layer with different soil hydraulic properties, and hysteresis to mention a few. While the uncertainties in this analysis may have contributed to the drastic conclusion, the severe reduction in groundwater recharge as a result of land use change in the Sand Hills should attract the attentions of water resources managers, who will need to consider management actions, such as identifying tree species that are less water intensive, optimum plantation density, and adaptive forest management activities (e.g. clearing and thinning) directed at prolonging the vitality of the Nebraska Sand Hills and the long term sustainability of the High Plains Aquifer.

In the effort to combat CO_2 emissions and global climate change, many semi-arid grasslands have been identified as suitable for future forestation programs worldwide. This case study provides further evidence of the importance of grassland ecology to water resources, particularly to groundwater systems. Thus, the impact of these plantation efforts on water sustainability, especially considering uncertainties in future climate projections in semi-arid regions, must be thoroughly considered.

Conflicts of interest

None.

Acknowledgements

This work was supported by the USDA National Institute of Food and Agriculture, McIntire Stennis project 1008861. The authors would also like to thank the Forestry lab at the School of Natural Resources, particularly Jeremy Hiller and Dr. Tala Awada for providing us with several sets of long term data and continuous access to the plots at the Nebraska National Forest near Halsey.

References

Adane, Z.A., Gates, J.B., 2015. Determining the impacts of experimental forest plantation on groundwater recharge in the Nebraska Sand Hills (USA) using chloride and sulfate. Hydrogeol. J. 23, 81–94. http://dx.doi.org/10.1007/s10040-014-1181-6.

Adane, Z.A., Nasta, P., Gates, J.B., 2017. Links between soil hydrophobicity and groundwater recharge under plantations in a sandy grassland setting, Nebraska Sand Hills USA. For. Sci. 64 (4), 388–401. http://dx.doi.org/10.5849/FS-2016-137.

Allen, A., Chapman, D., 2001. Impacts of afforestation on groundwater resources an quality. Hydrogeol. J. 9, 390–400. http://dx.doi.org/10.1007/s100400100148.

Bellot, J., Sanchez, J.R., Chirino, E., Hernandez, N., Abdelli, F., Martinez, J.M., 1999. Effect of different vegetation type cover effects on the soil water balance in a semi-arid areas of south eastern Spain. Phys. Chem. Earth (B) 24, 353–357.

Billesbach, D.P., Arkebauer, T.J., 2012. First long-term, direct measurements of evapotranspiration and surface water balance in the Nebraska Sand Hills. Agric. For. Meteorol. 156, 104–110. http://dx.doi.org/10.1016/j.agrformet.2012.01.001.

Bond, W.J., 2016. Ancient grasslands at risk. Science 351, 120–122.

Bosch, J.M., Hewlett, J.D., 1982. A review of catchment experiments to determine the effect of vegetation changes on water yield and evapotranspiration. J. Hydrol. 55, 3–23. http://dx.doi.org/10.1016/0022-1694(82)90117-2.
Bréda, N., 2003. Ground-based measurements of leaf area index: a review of methods, instruments and current controversies. J. Exp. Bot. 54, 2403–2417.
Brown, A.E., Western, A.W., McMahon, T.A., Zhang, L., 2013. Impact of forest cover changes on annual streamflow and flow duration curves. J. Hydrol. 483, 39–50. http://dx.doi.org/10.1016/j.jhydrol.2012.12.031.
Bruun, T.B., Elberling, B., de Neergaard, a., Magid, J., 2013. Organic carbon dynamics in different soil types after conversion of forest to agriculture. L. Degrad. Dev. 283http://dx.doi.org/10.1002/ldr.2205. n/a-n/a.
Burke, I.C., Yonker, C.M., Parton, W.J., Cole, C.V., Schimel, D.S., Flach, K., 1989. Texture, climate, and cultivation effects on soil organic matter content in U.S. grassland soils. Soil Sci. Soc. Am. J. 53, 800. http://dx.doi.org/10.2136/sssaj1989.03615995005300030029x.
Calder, I.R., Newson, M.D., 1980. The Effects of Afforestation on Water Resources in Scotland. In: Land Assessment in Scotland. Proc Symp Roy Geogr Soc Edinburgh. pp 51–62.
Calder, I.R., Rosier, P.T.W., Prasanna, K.T., Parameswarappa, S., 1997. Eucalyptus water use greater than rainfall input – a possible explanation from southern India. Hydrol. Earth Syst. Sci. 1, 249–256.
Calder, I.R., 2003. Impact of lowland forests in England on water resources: application of the Hydrological Land Use Change (HYLUC) model. Water Resour. Res. 39, 1–10. http://dx.doi.org/10.1029/2003WR002042.
Carsel, R.F., Parish, R.S., 1988. Developing joint probability distributions of soil water retention characteristics. Water Resour. Res. 24 (5), 75–769.
Crosbie, R.S., Scanlon, B.R., Mpelasoka, F.S., Reedy, R.C., Gates, J.B., Zhang, L., 2013. Potential climate change effects on groundwater recharge in the High Plains Aquifer, USA. Water Resour. Res. 49, 3936–3951. http://dx.doi.org/10.1002/wrcr.20292.
Eggemeyer, K.D., Awada, T., Harvey, F.E., Wedin, D.A., Zhou, X., Zanner, C.W., 2009. Seasonal changes in depth of water uptake for encroaching trees Juniperus virginiana and Pinus ponderosa and two dominant C4 grasses in a semiarid grassland. Tree Physiol. 29, 157–169. http://dx.doi.org/10.1093/treephys/tpn019.
Elmhagen, B., Eriksson, O., Lindborg, R., 2015. Implications of climate and land-use change for landscape processes, biodiversity, ecosystem services, and governance. Ambio 44. http://dx.doi.org/10.1007/s13280-014-0596-6.
FAO, 2005a. Global Forest Resources Assessment of 2005: porgress towards sustainable forest management. Forestry Paper 47. FAO, Rome.
FAO, 2005b. Grasslands of the world: grasslands of Central North America, prepared by Pieper R.D. Plant Production and Protection Series No. 34. FAO, Rome, pp. 221–251.
Farrington, P., Bartle, G.A., 1991. Recharge beneath a Banksia woodland and a Pinus pinaster plantation on coastal deep sands in south Western Australia. For. Ecol. Manag. 40, 101–118. http://dx.doi.org/10.1016/0378-1127(91)90096-E.
Feddes, R.A., Hoff, H., Bruen, M., Dawson, T., De Rosnay, P., Dirmeyer, P., Jackson, R.B., Kabat, P., Kleidon, A., Lilly, A., Pitman, A.J., 2001. Modeling root water uptake in hydrological and climate models. Bull. Am. Meteorol. Soc. 82, 2797–2809. http://dx.doi.org/10.1175/1520-0477(2001)082<2797:MRWUIH>2.3.CO;2.
Gates, J.B., Scanlon, B.R., Mu, X., Zhang, L., 2011. Impacts of soil conservation on groundwater recharge in the semi-arid Loess Plateau, China. Hydrogeol. J. 19, 865–875. http://dx.doi.org/10.1007/s10040-011-0716-3.
Ghimire, C.P., Bruijnzeel, L.A., Lubczynski, M.W., Bonell, M., 2012. Rainfall interception by natural and planted forests in the Middle Mountains of Central Nepal. J. Hydrol. 475, 270–280. http://dx.doi.org/10.1016/j.jhydrol.2012.09.051.
van Genuchten, M.T., 1980. A closed-form equation for predicting the hydraulic conductivity of unsaturated soils1. Soil Sci. Soc. Am. J. 44 (5), 892–898. http://dx.doi.org/10.2136/sssaj1980.03615995004400050002x.
Hargreaves, G.H., Allen, R.G., 2003. History and evaluation of Hargreaves evapotranspiration equation. J. Irrig. Drain. Eng. 129, 53–63. http://dx.doi.org/10.1061/(ASCE)0733-9437(2003)129:1(53).
He, Y., Guo, X., Wilmshurst, J.F., 2007. Comparison of different methods for measuring leaf area index in a mixed grassland. Can. J. Plant Sci. 87, 803–813.
Hellerich, J.A., 2006. Influence of Afforestation and Hillslope Position on Soil Carbon Dynamics in the Nebraska Sand Hills M.Sc. Thesis. University of Nebraska-Lincoln, USA, pp. 1–97.
Holmes, J.W., Colville, J.S., 1970a. Grassland hydrology in a karstic region in South Australia. J. Hydrol. 10, 38–58.
Holmes, J.W., Colville, J.S., 1970b. Forest hydrology in a karstic region in South Australia. J. Hydrol. 10, 59–74.
Huang, T., Pang, Z., 2011. Estimating groundwater recharge following land-use change using chloride mass balance of soil profiles: a case study at Guyuan and Xifeng in the Loess Plateau of China. Hydrogeol. J. 19, 177–186. http://dx.doi.org/10.1007/s10040-010-0643-8.
Huxman, T.E., Wilcox, B.P., Breshears, D.D., Scott, R.L., Snyder, K.A., Small, E.E., Hultine, K., Pockman, W.T., Jackson, R.B., 2005. Ecohydrological implications of woody plant encroachment. Ecology. pp. 308–319. http://dx.doi.org/10.1890/03-0583.
James, S.E., Pärtel, M., Wilson, S.D., Peltzer, D.A., 2003. Temporal heterogeneity of soil moisture in grassland and forest. J. Ecol. 91, 234–239. http://dx.doi.org/10.1046/j.1365-2745.2003.00758.x.
Kajiura, M., Etori, Y., Tange, T., 2012. Water condition control of in situ soil water repellency: an observational study from a hillslope in a Japanese humid-temperate forest. Hydrol. Process. 26, 3070–3078. http://dx.doi.org/10.1002/hyp.8310.
Kelliher, F.M., Leuning, R., Schulze, E.D., 1993. Evaporation and canopy characteristics of coniferous forests and grasslands. Oecologia 95, 153–163. http://dx.doi.org/10.1007/BF00323485.
Kettler, T.A., John, W., Doran, W., Gilbert, T.L., 2001. Simplified method for soil particle-size determination to accompany soil-quality analyses. Soil Sci. Soc. Am. J. 65, 849–852.
Klopatek, J.M., Olson, R.J., Emerson, C.L., Joness, J.L., 1979. Land-use conflicts with natural vegetation in the United States. Environ. Conserv. 6, 191–199.
Laloy, E., Vrugt, J.a., 2012. High-dimensional posterior exploration of hydrologic models using multiple-try DREAM(ZS) and high-performance computing. Water Resour. Res. 48, 1–18. http://dx.doi.org/10.1029/2011WR010608.
Longobardi, P., Montenegro, A., Beltrami, H., Eby, M., 2016. Deforestation induced climate change: effects of spatial scale. PLoS One 11. http://dx.doi.org/10.1371/journal.pone.0153357.
Maupin, M.a., Barber, N.L., 2005. Estimated Withdrawals from Principal Aquifers in the United States, 2000, US Geological Survey Circular 1279.
McCleery, D.W., 1992. American Forests: A History of Resiliency and Recovery. USDA Forest Service and Forest History Society, Durham, USA, pp. 27–31.
McMahon, P.B., Dennehy, K.F., Bruce, B.W., Böhlke, J.K., Michel, R.L., Gurdak, J.J., Hurlbut, D.B., 2006. Storage and transit time of chemicals in thick unsaturated zones under rangeland and irrigated cropland, High Plains, United States. Water Resour. Res. 42. http://dx.doi.org/10.1029/2005WR004417.
Miao, X.D., Mason, J.A., Johnson, W.C., Wang, H., 2007. High-resolution proxy record of holocene climate from a loess section in southwestern Nebraska, USA. Palaeogeogr. Palaeoclimatol. Palaeoecol. 245, 368–381.
Moradkhani, H., Sorooshian, S., Gupta, H.V., Houser, P.R., 2005. Dual state-parameter estimation of hydrological models using ensemble Kalman filter. Adv. Water Resour. 28, 135–147. http://dx.doi.org/10.1016/j.advwatres.2004.09.002.
Mualem, Y., 1976. A new model for predicting the hydraulic conductivity of unsaturated porous media. Water Resour. Res. 12, 513–522. http://dx.doi.org/10.1029/WR012i003p00513.
Nasi, R., Wunder, S., Campos, J.J.A., 2002. Forest Ecosystem Services: can They Pay Our Way Out of Deforestation? Fondo Glob. para el Medio Ambient, pp. 1–11.
Nasta, P., Gates, J.B., 2013. Plot-scale modeling of soil water dynamics and impacts of drought conditions beneath rainfed maize in Eastern Nebraska. Agric. Water Manag. 128, 120–130. http://dx.doi.org/10.1016/j.agwat.2013.06.021.
Nasta, P., Romano, N., 2016. Use of a flux-based field capacity criterion to identify effective hydraulic parameters of layered soil profiles subjected to synthetic drainage experiments. Water Resour. Res. 52, 566–584. http://dx.doi.org/10.1002/2015WR016979.
Ochoa-Quintero, J.M., Gardner, T.A., Rosa, I., de Barros Ferraz, S.F., Sutherland, W.J., 2015. Thresholds of species loss in Amazonian deforestation frontier landscapes. Conserv. Biol. 29, 440–451. http://dx.doi.org/10.1111/cobi.12446.
Owens, M.K., Lyons, R.K., Alejandro, C.L., 2006. Rainfall partitioning within semiarid juniper communities: effects of event size and canopy cover. Hydrol. Process. 20, 3179–3189. http://dx.doi.org/10.1002/hyp.6326.

Ozalp, M., Erdogan Yuksel, E., Yuksek, T., 2016. Soil property changes after conversion from forest to pasture in Mount Sacinka, Artvin, Turkey. Land Degrad. Dev. 27, 1007–1017. http://dx.doi.org/10.1002/ldr.2353.

Ritchie, J.T., 1972. Model for predicting evaporation from a row crop with incomplete cover. Water Resour. Res. 8, 1204–1213. http://dx.doi.org/10.1029/WR008i005p01204.

Robbins, C.R., 2005. Analyses of High Resolution Hyperspectral Imager for Characterization of Ponderosa Pine Woodlands M.S. Thesis. University of Nebraska-Lincoln, USA, pp. p 1–62.

Scanlon, B.R., Jolly, I., Sophocleous, M., Zhang, L., 2007. Global impacts of conversions from natural to agricultural ecosystems on water resources: quantity versus quality. Water Resour. Res. 43, 1–18.

Scanlon, B.R., Stonestrom, D.A., Reedy, R.C., Leaney, F.W., Gates, J.B., Cresswell, R.G., 2009. Inventories and mobilization of unsaturated zone sulfate, fluoride, and chloride related to land use change in semiarid regions, southwestern United States and Australia. Water Resour. Res. 45, 1–17.

Scanlon, B.R., Faunt, C.C., Longuevergne, L., Reedy, R.C., Alley, W.M., McGuire, V.L., McMahon, P.B., 2012. Groundwater depletion and sustainability of irrigation in the US High Plains and Central Valley. Proc. Natl. Acad. Sci. 109, 9320–9325. http://dx.doi.org/10.1073/pnas.1200311109.

Schilling, K.E., Jha, M.K., Zhang, Y.-K., Gassman, P.W., Wolter, C.F., 2008. Impact of land use and land cover change on the water balance of a large agricultural watershed: historical effects and future directions. Water Resour. Res. 44, 1–12. http://dx.doi.org/10.1029/2007WR006644.

Seppelt, R., Dormann, C.F., Eppink, F.V., Lautenbach, S., Schmidt, S., 2011. A quantitative review of ecosystem service studies: approaches shortcomings, and the road ahead. J. Appl. Ecol. 48, 630–636.

Sharma, M.L., Farrington, P., Fernie, M., 1983. Localised groundwater recharge on the Gnangara Mound, Western Australia. In: Int. Conf. on Groundwater and Man. Sydney, 5–9 December. Conf..

Sieg, C.H., Flather, C.H., McCanny, S., 1999. Recent biodiversity patterns in the great plains: implications for restoration and management. Gt. Plains Res. 9, 277–313.

Simic, A., Fernandes, R., Wang, S., 2014. Assessing the impact of leaf area index on evapotranspiration and groundwater recharge across a shallow water region for diverse land cover and soil properties. J. Water Resour. Hydraul. Eng. 3, 60–73.

Šimůnek, J., Šejna, M., Saito, H., Sakai, M., van Genuchten, M.T., 2008. The HYDRUS-1D Software Package for Simulating the One-dimensional Movement of Water, Heat, and Multiple Solutes in Variably-saturated Media. Version 4.0, HYDRUS Software Series 4. Department of Environmental Sciences, University of California Riverside, Riverside, CA, USA.

Spracklen, D.V., Garcia-Carreras, L., 2015. The impact of Amazonian deforestation on Amazon basin rainfall. Geophys. Res. Lett. 42, 9546–9552. http://dx.doi.org/10.1002/2015GL066063.

Starks, P.J., Venuto, B.C., Dugas, W.A., Kiniry, J., 2014. Measurements of canopy interception and transpiration of eastern redcedar grown in open environments. Environ. Nat. Resour. Res. 4, 103–122. http://dx.doi.org/10.5539/enrr.v4n3p103.

Stogsdili Jr., W.R., Wittwer, R.F., Hennessey, T.C., Dougherty, P.M., 1992. Water use in thinned loblolly pine plantations. For. Ecol. Manag. 50, 233–245. http://dx.doi.org/10.1016/0378-1127(92)90338-A.

Szilagyi, J., Zlotnik, V.A., Gates, J.B., Jozsa, J., 2011. Mapping mean annual groundwater recharge in the Nebraska Sand Hills, USA. Hydrogeol. J. 19, 1503–1513. http://dx.doi.org/10.1007/s10040-011-0769-3.

Terrell, B.L., Johnson, P.N., Segarra, E., 2002. Ogallala aquifer depletion: economic impact on the Texas high plains. Water Policy 4, 33–46. http://dx.doi.org/10.1016/S1366-7017(02)00009-0.

Valante, F., David, J.S., Gash, J.H.C., 1997. Modelling interception loss for two sparse eucalypt and pine forests in central Portugal using reformulated Rutter and Gash analytical models. J. Hydrol. 190, 141–162. http://dx.doi.org/10.1016/S0022-1694(96)03066-1.

Vrugt, J. a., Bouten, W., Gupta, H.V., Hopmans, J.W., 2003. Toward improved identifiability of soil hydraulic parameters: on the selection of a suitable parametric model. Vadose Zone J. 2, 98–113. http://dx.doi.org/10.2113/2.1.98.

Vrugt, J.A., ter Braak, C.J.F., Clark, M.P., Hyman, J.M., Robinson, B.A., 2008. Treatment of input uncertainty in hydrologic modeling: doing hydrology backwards with Markov chain Monte Carlo simulation. Water Resour. Res. 44http://dx.doi.org/10.1029/2007WR006720. W00B09.

Vrugt, J.A., 2016. Markov chain Monte Carlo simulation using the DREAM software package: theory, concepts, and MATLAB implementation. Environ. Model. Softw. 75, 273–316. http://dx.doi.org/10.1016/j.envsoft.2015.08.013.

Wöhling, T., Vrugt, J.A., 2011. Multi-response multi-layer vadose zone model calibration using Markov chain Monte Carlo simulation and field water retention data. Water Resour. Res. 47http://dx.doi.org/10.1029/2010WR009265. W04510.

Wang, T., Wedin, D., Zlotnik, V.A., 2009. Field evidence of a negative correlation between saturated hydraulic conductivity and soil carbon in a sandy soil. Water Resour. Res. 45 W07503.

Wang, T., Franz, T.E., Yue, W., Szilagyi, J., Zlotnik, V.A., You, J., Chen, X., Shulski, M.D., Young, A., 2016. Feasibility analysis of using inverse modeling for estimating natural groundwater recharge from a large-scale soil moisture monitoring network. J. Hydrol. 533, 250–265. http://dx.doi.org/10.1016/j.jhydrol.2015.12.019.

Yang, L., Wei, W., Chen, L., Mob, B., 2012. Response of deep soil moisture to land use and afforestation in the semi-arid Loess Plateau, China. J. Hydrol. 475, 111–122.

Zhang, L., Dawes, W.R., Walker, G.R., 2001. Response of mean annual evapotranspiration to vegetation changes at catchment scale. Water Resour. Res. 37, 701–708. http://dx.doi.org/10.1029/2000WR900325.